Photon-induced L-subshell Auger decay for elements in the atomic number range $28 \leq Z \leq 96$

A. Meddah[1,2], A. Kahoul[1,2*], F. Parente[3], S. Daoudi[1,2], J.M. Sampaio[4,5], J.P. Marques[4,5], S. Croft[6], A. Favalli[7,8], E. Cengiz[9], Y. Kasri[10,11]

[1]*Department of Matter Sciences, Faculty of Sciences and Technology, Mohamed El Bachir El Ibrahimi University, Bordj-Bou-Arreridj 34030, Algeria.*
[2]*Laboratory of Materials Physics, Radiation and Nanostructures (LPMRN), Faculty of Sciences and Technology, Mohamed El Bachir El Ibrahimi University, Bordj-Bou-Arreridj 34030, Algeria.*
[3]*Laboratory of Instrumentation, Biomedical Engineering and Radiation Physics (LIBPhys-UNL), Department of Physics, NOVA School of Science and Technology, NOVA University Lisbon, 2829-516 Caparica, Portugal.*
[4]*LIP – Laboratório de Instrumentação e Física Experimental de Partículas, Av. Prof. Gama Pinto 2, 1649-003 Lisboa, Portugal.*
[5]*Faculdade de Ciências da Universidade de Lisboa, Campo Grande, C8, 1749-016 Lisboa, Portugal.*
[6]*School of Engineering, Faculty of Science of Technology, Nuclear Science & Engineering Research Group, Lancaster University, Bailrigg, Lancaster, LA1 4YW, United Kingdom.*
[7]*European Commission, Joint Research Centre, Ispra, I-21027, Italy.*
[8]*Los Alamos National Laboratory, P.O. Box 1663, Los Alamos, NM 87545, USA.*
[9]*Department of Fundamental Sciences, Rafet Kayış Engineering Faculty, Alanya Alaaddin Keykubat University, 07425 Alanya/Antalya, Türkiye.*
[10]*Physics Department, Faculty of Sciences, University of Mohamed Boudiaf, 28000 M'sila, Algeria.*
[11]*Theoretical Physics Laboratory, Faculty of Exact Sciences, University of Bejaia, 06000 Bejaia, Algeria.*

*Corresponding author. Tel. /Fax (+213) 035862230.
E-mail address: *a.kahoul@univ-bba.dz*

Abstract: This study investigates Auger decay processes by analyzing experimental data to derive key parameters—denoted as a_1, a_2, and a_3—that describe transition probabilities. A fitting methodology was employed to model the behavior of Auger decay rates as functions of specific variables, enabling the development of simple mathematical representations for various atomic levels. To enhance the predictive capability of the model, numerical interpolation was applied between gaps in the available data points, allowing for the estimation of transition probabilities in regions lacking direct measurements. This approach highlights the value of combining fitting and interpolation techniques to construct comprehensive databases of Auger transitions. In addition, new theoretical calculations based on the multi-configuration Dirac–Fock method have been carried out for selected elements and are presented in this work. Finally, the experimentally and theoretically derived a_i subshell Auger decay rates are compared with other experimental results and empirical values reported in the literature.

Keywords: Atomic parameters, Auger decay transition, Empirical and MCDF calculation.

1. Introduction

Analytical methods based on X-ray fluorescence (XRF) play a critical role in a wide range of practical applications, including atomic physics, surface chemical analysis, medical research and treatments (such as cancer therapy), and industrial irradiation processing. Among the fundamental parameters in atomic physics are fluorescence yields, which are essential for the quantitative analysis of materials. They also serve in determining quantities such as ionization and excitation cross sections from detected spectra and are crucial for calculating X-ray production cross sections (Sahnoune et al., 2020).

This paper focuses on Auger decays and the empirical determination and refinement of associated values for a variety of elements. Auger processes take place when an inner energy-level vacancy in an ionized atom is filled resulting in the emission of characteristic electrons and photons. Our focus here is solely on the X-ray emissions.Numerous efforts have been made to measure and model L-shell Auger decay, either through theoretical approaches or by fitting experimental data with empirical formulas across a broad range of atomic numbers.

Krause (1979) provided a foundational set of semi-empirical and theoretical estimates for Auger yields in elements with atomic numbers $12 \leq Z \leq 110$. His work was pivotal in standardizing radiative and non-radiative transition values and contributed to a comprehensive database for studying L-shell dynamics in heavy elements. Earlier, McGuire (1972) computed Auger, Coster–Kronig, super Coster–Kronig, and radiative transition rates using non-relativistic Hartree–Fock–Slater (HFS) wave functions via the Herman–Skillman code (Herman and Skillman, 1963) for elements within $20 \leq Z \leq 90$. Öz et al. (2000) carried out a detailed analysis of Auger yields for elements with atomic numbers from $_{59}$La to $_{85}$Bi, utilizing analytical methods and mathematical models fitted to radiative and non-radiative yield data. Later, Öz et

al. (2001) extended this work by comparing inferred values for elements in the range $59 \leq Z \leq 90$ with theoretical predictions, previous semi-empirical values, and measured Coster–Kronig yields. Özdemir et al. (2003) reported measurements of Auger yields from the L_1, L_2 and L_3 sub-levels (denoted as a_1, a_2, and a_3) for elements with atomic numbers between $_{55}$Cs and $_{92}$U. Experimental fluorescence yields (w_1, w_2, w_3) and Coster–Kronig transition probabilities (f_{12}, f_{13}, f_{23}) were used to calculate Auger yields through specific relationships, and results were fitted as third-order polynomials in atomic number. These data provided a valuable benchmark or reference set for improving agreement between theoretical and experimental Auger yields in heavy elements. Kaur et al. (2016) employed a polynomial fitting approach to estimate Coster–Kronig transition probabilities as functions of atomic number, based on experimental data obtained via synchrotron radiation. Their fitting equations followed a second-order logarithmic form and exhibited good agreement with experimental results.

Kahoul et al. (2011) presented empirical K-shell fluorescence yields by fitting available experimental data using polynomial functions, although the exact quantity being fitted was not explicitly defined. A third-order polynomial of the form $\sum_{n=0}^{3} b_n Z^n$ was found to best represent the data. In a follow-up study, Kahoul et al. (2012) derived empirical K-shell fluorescence yields by fitting both weighted and unweighted mean values of experimental data collected between 1960 and 2011. Dogan et al. (2013) adopted a similar method for their empirical analysis. Kup-Aylikci et al. (2011) and Aylikci et al. (2015) also employed this empirical approach to calculate empirical K-shell fluorescence yields, while Daoudi et al. (2015) used interpolation of all available experimental data to derive average values through analytical functions of Z. More recently, Sahnoune et al. (2020) applied similar analytical techniques to estimate empirical values. While the influence of the chemical environment on Auger transitions is generally considered minimal, certain external conditions—such as temperature, pressure, and surrounding materials—can subtly affect transition rates or the stability of energy

levels. For instance, some studies (e.g., Özdemir et al., 2016) have reported that elevated temperatures may increase intra-atomic electron mobility, potentially altering transition probabilities.

In the present study, we determine empirical values for the Auger decay parameters a_1, a_2, and a_3 using the recent comprehensive experimental database from our previously published work (Meddah et al., 2025). We also present new theoretical calculations for selected elements based on the multi-configuration Dirac–Fock (MCDF) method which is a principled or physics informed computational technique.

2. Calculation procedure of empirical Auger Decay transitions

The database taken as the starting point in this work is described in our recently published experimental compilation (Meddah et al., 2025). In this investigation, we derived the empirical Auger decay parameters a_1, a_2, and a_3 by directly interpolating the experimental data. The experimental values of Auger decay were plotted as functions of atomic number *Z*, as shown in Fig. 1, Fig. 2, and Fig. 3, extracted from the Meddah et al. (2025) database. The empirical value of a_1 was calculated for the first time using 105 data points, representing a pioneering use of such an extensive dataset. Similarly, a_2 was determined using 146 data points, and a_3 was calculated using 131 data points—both for the first time at this scale.

To ensure reliable empirical Auger decay values, the atomic number range for a_1 was divided into three *Z*-groups: low *Z* region: $40 \leq Z \leq 47$, medium and high *Z* region: $50 \leq Z \leq 74$ and high *Z* region: $75 \leq Z \leq 93$. For a_2 and a_3, a single atomic number range was used: $40 \leq Z \leq 96$. This grouping approach was guided by the observed trends in Auger decay transition values reported by Krause (1979) and Özdemir (2003).

The general form of the polynomial functions used for the fitting process are as follows:

$$(a_1, a_2, a_3)_{emp} = \sum_{i=0}^{n} b_i Z^i = f(Z) \quad (1)$$

The fitted models are represented by solid lines in Figs. 1–3. The corresponding fitting coefficients b_i are summarized in Table 1 and the derived empirical values are listed in Tables 2–4. The overall deviation between the calculated empirical values of a_1, a_2, and a_3 and the corresponding experimental data is quantified using the root-mean-square error, ($\varepsilon_{\mathrm{RMS}}$), calculated according to the following expression (Kahoul et al., 2011):

$$\varepsilon_{RMS} = \left[\sum_{j=1}^{N} \frac{1}{N}\left(\frac{\chi_{j\mathrm{expt}} - \chi_{j\mathrm{calc}}}{\chi_{j\mathrm{calc}}}\right)^2\right]^{\frac{1}{2}} \quad (2)$$

where *N* represents the total number of experimental data points, χ_{expt} denotes the experimental a_1, a_2, and a_3 and χ_{calc} signifies the a_1, a_2, and a_3 Auger decay parameter calculated using the polynomial fits to the respective data sets. The total $\varepsilon_{\mathrm{RMS}}$ for the empirical results are provided in Table 1 for each transition.

The Auger process is directly influenced by the presence of Coster–Kronig transitions, which result in an average deviation ε_{RMS} in the value of a_1 due to the combined effects of the f_{12} and f_{13} transitions. For a_2, a relatively small deviation ε_{RMS} was observed, which can be attributed to the influence of a single Coster–Kronig transition, f_{23}.

In contrast, a_3 exhibited excellent consistency, likely due to the absence of Coster–Kronig transitions.

3. Relativistic calculations

a_1, a_2, and a_3 Auger decay rates were calculated using the multiconfiguration Dirac–Fock (MCDF) method, as implemented by Desclaux (1975) and further developed by Indelicato (Indelicato and Desclaux, 1990). The MCDFGME code solves the Dirac–Coulomb–Breit

Hamiltonian and was executed in single-configuration mode using custom software. This approach was chosen because the approximation typically used for calculating non-radiative decay rates is not compatible with optimized level (OL) calculations that involve bonded orbitals (Gerra et al., 2018).

The theoretical values, calculated for thirteen elements—$_{28}$Ni, $_{29}$Cu, $_{30}$Zn, $_{32}$Ge, $_{33}$As, $_{34}$Se, $_{36}$Kr, $_{48}$Cd, $_{50}$Sn, $_{52}$Te, $_{80}$Hg, $_{83}$Bi, $_{86}$Rn—are reported to three significant figures in Tables 2–4 for a_1, a_2, and a_3 Auger decay process, respectively. These tables demonstrate excellent agreement between the empirical results and the theoretical predictions obtained using the MCDF method, outperforming other available theoretical approaches.

Results and discussion:

The present calculation of Auger decay parameters covers all elements in the range $28 \leq Z \leq 98$. In addition, theoretical values for thirteen selected elements $_{28}$Ni, $_{29}$Cu, $_{30}$Zn, $_{32}$Ge, $_{33}$As, $_{34}$Se, $_{36}$Kr, $_{48}$Cd, $_{50}$Sn, $_{52}$Te, $_{80}$Hg, $_{83}$Bi, $_{86}$Rn were calculated using the MCDFGME code. These results are provided numerically in Tables 2–4. For comprehensive comparison, the tables also include the semi-empirical fits of Krause (1979), Özdemir (2003), and Öz et al. (2000), along with experimental measurements from Özdemir (2003) and Öz et al. (2000).

To facilitate comparison of our empirical a_1 Auger decay values with these semi-empirical, fitted, and experimental results, all values are plotted as a function of atomic number in Figures 1–3. Overall, our empirical Auger decay values—calculated using Eq. (1)—exhibit good agreement with previously reported data. While slight deviations are observed between our empirical values and those of Krause (1979) in the range $40 \leq Z \leq 98$, particularly for the lanthanides, the agreement is notably strong.

In contrast, the experimental data from Özdemir et al. (2003) show greater discrepancies, especially for heavier elements. Our empirical data generally agree with Krause (1979) within a deviation range of 1.0% to 10%, except for a few values where deviations reach up to about

30%. When compared with the values from Öz et al. (2000) and Özdemir et al. (2003), the deviations span from approximately 0.0% to 18%, with the majority of elements falling below 14%.

However, notable discrepancies are observed for specific heavy elements, particularly $_{76}$Os, $_{77}$Ir, $_{78}$Pt, $_{79}$Au, $_{80}$Hg, $_{81}$Tl, $_{82}$Pb and $_{83}$Bi, as seen in Figure 1. In the atomic number range $86 \leq Z \leq 96$, our theoretical values differ modestly from those of Krause (1979), Özdemir et al. (2003), and Öz et al. (2000), with deviations ranging from roughly 2.7% to 37%. For lighter elements ($28 \leq Z \leq 36$), Krause's values show larger discrepancies, with some deviations exceeding 50%. Notably, our theoretical results show very good agreement with experimental values for most elements, with deviations ranging from 0.81% to 4.6%, except for element $_{48}$Cd, which shows a higher deviation of about 37%. In this context, the relative deviation (RD) is used to quantify the difference between empirical and reference values and is calculated using the following formula:

$$\mathrm{RD}(\%) = \left|\left((a_1)_{\mathrm{exp}} - (a_1)_{\mathrm{emp}}\right)/(a_1)_{\mathrm{emp}}\right| \times 100.$$

Regarding the empirical a_2 Auger decay (a_2-*emp*), Figure 5 illustrates its variation as a function of atomic number (*Z*). This comparison includes semi-empirical values and fitted data from Krause (1979), Özdemir (2003), and Öz et al. (2000). Additionally, experimental measurements reported by Özdemir (2003) and Öz et al. (2000) are incorporated into the same table for direct comparison. Our empirical values were calculated using Equation (1) for elements in the atomic number range $40 \leq Z \leq 98$. The results show that our empirical findings are in strong agreement with the semi-empirical values reported by Krause (1979), with relative deviations ranging from 0.0% to 13%. For most elements, the difference is particularly small—between 0.0% and 3.7%—with the exception of element $_{63}$Eu, which exhibits a deviation of 9.1%.

Comparison with experimental data also confirms a high level of consistency. The deviations between our empirical values and the experimental results range from 0.14% to 8.7% for Özdemir (2003), and from 0.15% to 3.6% for Öz et al. (2000).

As shown in Figure 5, our theoretical calculations exhibit a high level of agreement with previous works, with deviations ranging from approximately 1.6% to 6.0%. However, notable discrepancies are observed for specific elements: $_{36}$Kr, $_{48}$Cd, and $_{86}$Rn, with deviations of 9.4%, 15%, and 9.1%, respectively. Compared with the fitted values reported by Öz et al. (2000) and the experimental data from Öz et al. (2000) and Özdemir (2003), which show deviations in the range of 2.0% to 6.3%, our results align well—within a deviation range of 0.45% to 6.5%—except for element $_{48}$Cd, which shows a significant deviation of nearly 29%. Overall, the comparison between our empirical results and theoretical values confirms a good level of agreement.

In the case of the empirical a_3 Auger decay (a_3-*emp*), our results show strong consistency across the entire dataset. The relative differences compared to Krause (1979) range from 0.0% to 4.6%, while for Özdemir et al. (2003), they fall between 0.12% and 3.5%. Comparison with the experimental measurements reveals similarly high agreement: 0.26% to 2.9% for Öz et al. (2000), and 0.0% to 2.7% for Özdemir (2003).

It is worth emphasizing that the semi-empirical and fitted values from Krause (1979), Özdemir (2003), and Öz et al. (2000) closely match our theoretical results obtained using the MCDFGME code for elements in the range $40 \leq Z \leq 96$, with a maximum relative difference (RD) of just 4.4%. Our theoretical calculations are particularly close to our empirical values, with deviations not exceeding 0.73%.

Due to the absence of experimental data for elements $_{48}$Cd and $_{49}$In, extrapolation was used to estimate a_1 values. Additionally, we excluded a_1 values reported by Öz et al. (2000) for $_{73}$Ta, Borovoĭ et al. (2003) for $_{77}$Ir, Rich (1958) for $_{81}$Tl, and Weksler and Pinho (1973) as well as

Karttunen (1971) for $_{93}$Np and $_{96}$Cm, as these values were significantly higher than the rest of the dataset. Similarly, for a_2, the value provided by Byrne et al. (1968) for $_{92}$U was excluded due to a substantial deviation from expected trends.

4. Conclusion

This study focused on calculating empirical Auger decay parameters— a_1, a_2, and a_3—by interpolating experimental data extracted from established databases. In parallel, first-principles theoretical calculations were carried out using the multiconfiguration Dirac–Fock (MCDF) method for thirteen representative elements. The results demonstrate good overall agreement with findings from other research groups, highlighting the importance of integrating both empirical and theoretical approaches to coherently characterize the spectroscopic properties of materials over a wide dynamic range. The methodology used to calculate empirical Auger decay values produced reliable outcomes that can be readily incorporated into formulas and computer codes for computing X-ray ionization and production cross sections. By integrating these experimental benchmarks, our findings not only enhance the reliability and applicability of the data but also advance our overall understanding of spectroscopic properties across the periodic table. Several elements lacking experimental data were identified and several elements where agreement across experiments and evaluations is poor were noted. These should be targeted for future experimental redetermination.

5. Acknowledgments

We gratefully acknowledge the support of the Directorate General for Scientific Research and Technological Development (DGRSDT), Ministry of Higher Education and Scientific Research, Algeria. This work was carried out with the support of Mohamed El Bachir El Ibrahimi University under project (PRFU) No. B00L02UN340120230001. Additional support was provided by the Fundação para a Ciência e a Tecnologia (FCT), Portugal, through contracts UIDP/50007/2020 (LIP) and UID/FIS/04559/2020 (LIBPhys). S.C. warmly acknowledges financial support from Lancaster University, and A.F. gratefully acknowledges the support of the Joint Research Centre of the European Commission.

Figure caption:

Fig. 1. Distribution of the experimental a_{1_Exp}values as a function of the atomic number *Z.* The curve is the interpolation according to Eq. (1).

Fig. 2. Distribution of the experimental a_{2_Exp}values as a function of the atomic number *Z.* The curve is the interpolation according to Eq. (1).

Fig. 3. Distribution of the experimental a_{3_Exp}values as a function of the atomic number *Z.* The curve is the interpolation according to Eq. (1).

Fig. 4. The empirical values of the Auger decay parameter a_{1-emp} and the theoretical values (MCDF) compared to the experimental values from (Öz et al., 2000, Özdemir, 2003), Semi-empirical values of (Krause,1979) and the fitting values of (Öz et al., 2000) as a function of atomic number *Z.*

Fig. 5. The empirical values of the Auger decay parameter a_{2-emp} and the theoretical values (MCDF) compared to the experimental values from (Öz et al., 2000, Özdemir, 2003), Semi-empirical values of (Krause,1979) and the fitting values of (Öz et al., 2000) as a function of atomic number *Z.*

Fig. 6. The empirical values of the Auger decay parameter a_{3-emp} and the theoretical values (MCDF) compared to the experimental values from (Öz et al., 2000, Özdemir, 2003), Semi-empirical values of (Krause,1979) and the fitting values of (Öz et al., 2000) as a function of atomic number *Z.*

References

Aylikci, N. K., Aylikci, V., Kahoul, A., Tiraşoğlu, E. N., Karahan, I. H., & Cengiz, E. R. (2011). Effect of p H treatment on K-shell x-ray intensity ratios and K-shell x-ray-production cross sections in ZnCo alloys. *Phys. Rev* A, 84, 042509-10.

Aylikci, V., Kahoul, A., Kup Aylikci, N., Tiraşoğlu, E., Karahan, İ. H., Abassi, A., & Dogan, M. (2015). Empirical and semi-empirical interpolation of L X-ray fluorescence parameters for elements in the atomic range $50 \leq Z \leq 92$. *Radiat. Phys. Chem*. 106, 99-125.

Byrne, J., Gelletly, W., Ross, M.A., & Shaikh, F. (1968). Subshell yield measurements. *Phys. Rev.*, 170, 81–88.

Daoudi, S., Kahoul, A., Kup Aylikci, N., Sampaio, J. M., Marques, J. P., Aylikci, V., Sahnoune, Y., Kasri, Y., & Deghfel, B. (2020). Review of experimental photon-induced Kβ/Kα intensity ratios. *At. Data Nucl. Data Tables*, 132, 101308.

Desclaux, J. (1975). A multiconfiguration relativistic Dirac-Fock program. Comput. *Phys. Commun*. 9(1), 31-45.

Dogan, M., Tirasoglu, E., Karahan, İ. H., Aylikci, N. K., Aylikci, V., Kahoul, A., Serifoglu, O. (2013). Alloying effect on K X-ray intensity ratio and production cross section values of Zn and Cr in Zn Cr alloys. *Radiat. Phys*. Chem, 87, 6–15.

Guerra, M., Sampaio, J. M., Madeira, T. I., Parente, F., Indelicato, P., Marques, J. P., Santos, J. P., Hoszowska, J., Dousse, J.-Cl., Loperetti, L., Zeeshan, F., Müller, M.,

Unterumsberger, R., & Beckhoff, B. (2015). Theoretical and experimental determination of L -shell decay rates, line widths, and fluorescence yields in Ge. *Phys. Rev. A*. 92(2), 022507.

Guerra, M., Sampaio, J. M., Parente, F., Indelicato, P., Hönicke, P., Müller, M., Beckhoff, B., Marques, J. P., & Santos, J. P. (2018). Theoretical and experimental determination of K - and L -shell x-ray relaxation parameters in Ni. *Phys. Rev*. 97(4), 042501.

Herman F., & Skillman S. (1963). Atomic Structure Calculations, Prentice-Hall, Englewood Cliffs, New Jersey.

Indelicato, P., & Desclaux, J. P. (1990). Multiconfiguration Dirac-Fock calculations of transition energies with QED corrections in three-electron ions. *Phys. Rev*. A. 42(9), 5139–5149.

Kahoul, A., Aylikci, V., Kup, Aylikci, N., Cengiz, E., Apaydın, G. (2012). Updated database and new empirical values for K-shell fluorescence yields. Radiat. Phys. Chem. 81, 713-727.

Kahoul, A., Abassi, A., Deghfel, B., & Nekkab, M. (2011). K-shell fluorescence yields for elements with $6 \leq Z \leq 99$. *Radiat. Phys. Chem.*, 80, 369–377.

Kaur, G., Bansal, H., Tiwari, M. K., & Mittal, R. (2016). *L* Subshell fluorescent X-ray measurements to study CK transitions in the $66 \leq Z \leq 83$ region. *Pramana - J. Phys*, 87, 33.

Krause, M. O. (1979). Atomic radiative and radiationless yields for K and L shells. *J. Phys. Chem. Ref. Data*, 8, 307–327.

McGuire, E. J. (1972). Atomic M-shell Coster-Kronig, Auger, and radiative rates, and fluorescence yields for Ca-Th. *Phys. Rev A*, 5(3), 1043-1047.

Meddah, S., Kahoul, A., Parente, F., Daoudi, S., Marques, J. P., Sampaio, J. M., Croft, S., Favalli, A., Kasri, Y., Kup Aylikci, N., Aylikci, V., & Hamidani, A. (2025). L-subshell experimental Coster–Kronig probabilities and Auger decays for elements in the atomic number range $28 \leq Z \leq 100$. *Atomic Data and Nuclear Data Tables*, 164, 101731.

Öz, E., Ekinci, N., Özdemir, Y., Ertuğrul, M., Sahin, Y., & Erdogan, H. (2001). Measurement of atomic L shell Coster-Kronig yields (f_{12}, f_{23} and f_{13}) for some elements in the atomic number range $59 \leq Z \leq 90$. *J. Phys. B: At. Mol. Opt. Phys*, 34, 631-638.

Öz, E., Özdemir, Y., Ekinci, N., Ertugrul, M., Sahin, Y., & Erdogan, H. (2000). Measurement of atomic L shell fluorescence and Auger yields for some elements in the atomic number range $59 \leq Z \leq 85$. *Spectrochimica Acta Part B: Atomic Spectroscopy*, 55, 1869–1877.

Özdemir, Y., & Durak, R. (2003). L-subshell fluorescence yields (ω_1, ω_2 and ω_3) for elements in the atomic range $55 \leq Z \leq 68$ with a Si(Li) detector. *J. Quant. Spectrosc. Radiat. Transf.*, 77(2003), 95–103.

Özdemir, Y., Kavaz, E., Ahmadi, N., Ertuğrul, M., & Ekinci, N. (2016). Investigation of K X-ray intensity ratios of some 4d transition metals depending on the temperature. *Appl. Radiat. Isot*. 115, 147-154.

Sahnoune Y., Kahoul A., Daoudi S., Sampaio J.M., Aylikci N.K., Aylikci V., Aylikci V., Kasri Y., Deghfel B., Marques J.P., Medjadi D.E. (2020). Updated database, new empirical and theoretical values of average L shell fluorescence yields of elements with $23 \leq Z \leq 96$. *Radiat. Phys. Chem.* 166, 108495.

Sahnoune, Y., Kahoul, A., Kasri, Y., Deghfel, B., Medjadi, D. E., Khalfallah, F., Daoudi, S., Aylikçi, V., Küp Aylikçi, N., & Nekkab, M. (2016). L_1, L_2 , and L_3 subshell fluorescence yields : Updated database and new empirical values. *Radiat. Phys. Chem.* 125, 227-251.

Figure 01:

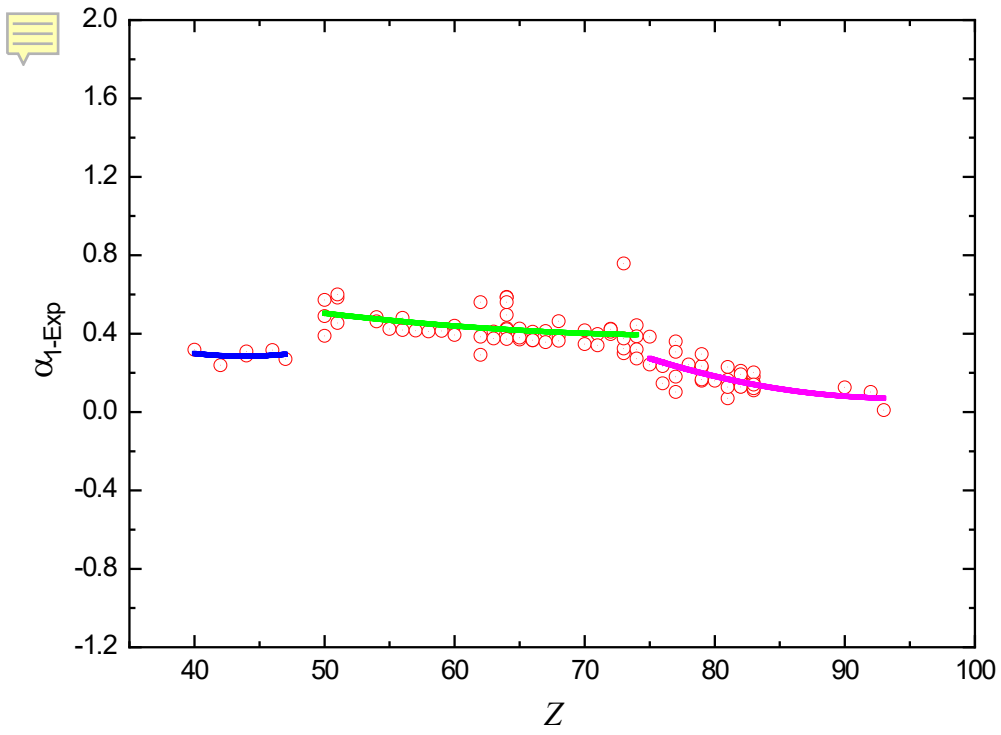

Figure 02:

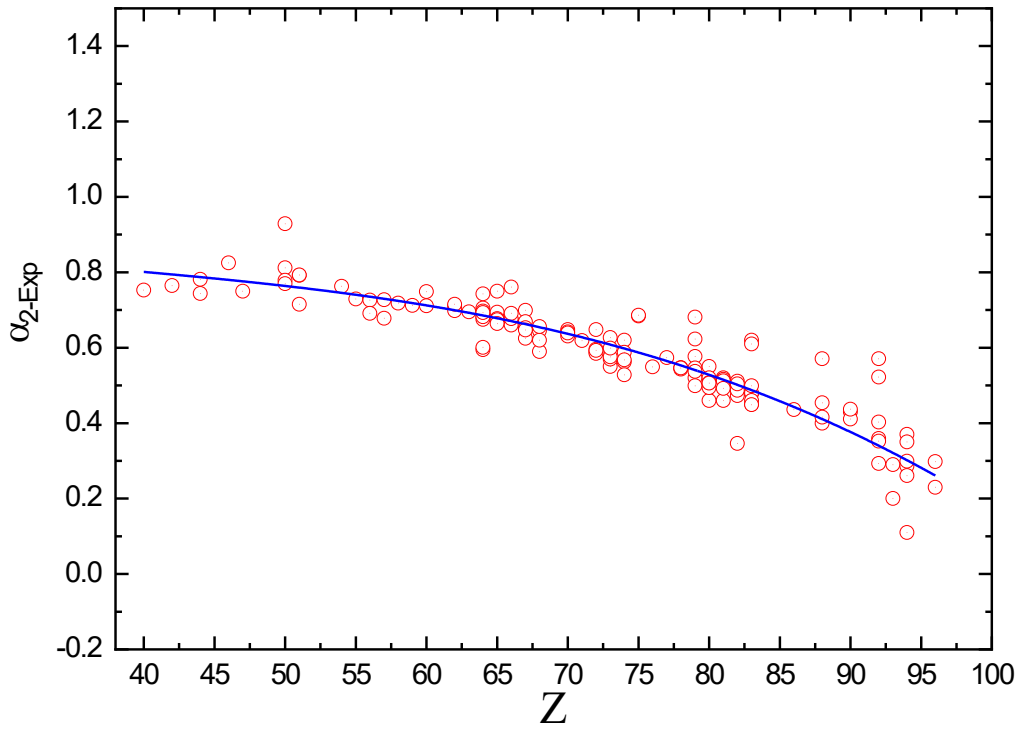
1.4
1.2
1.0
0.8
0.6
0.4
0.2
0.0
-0.2
$\alpha_{2\text{-Exp}}$
40
45
50
55
60
65
70
75
80
85
90
95
100
Z

Figure 03:

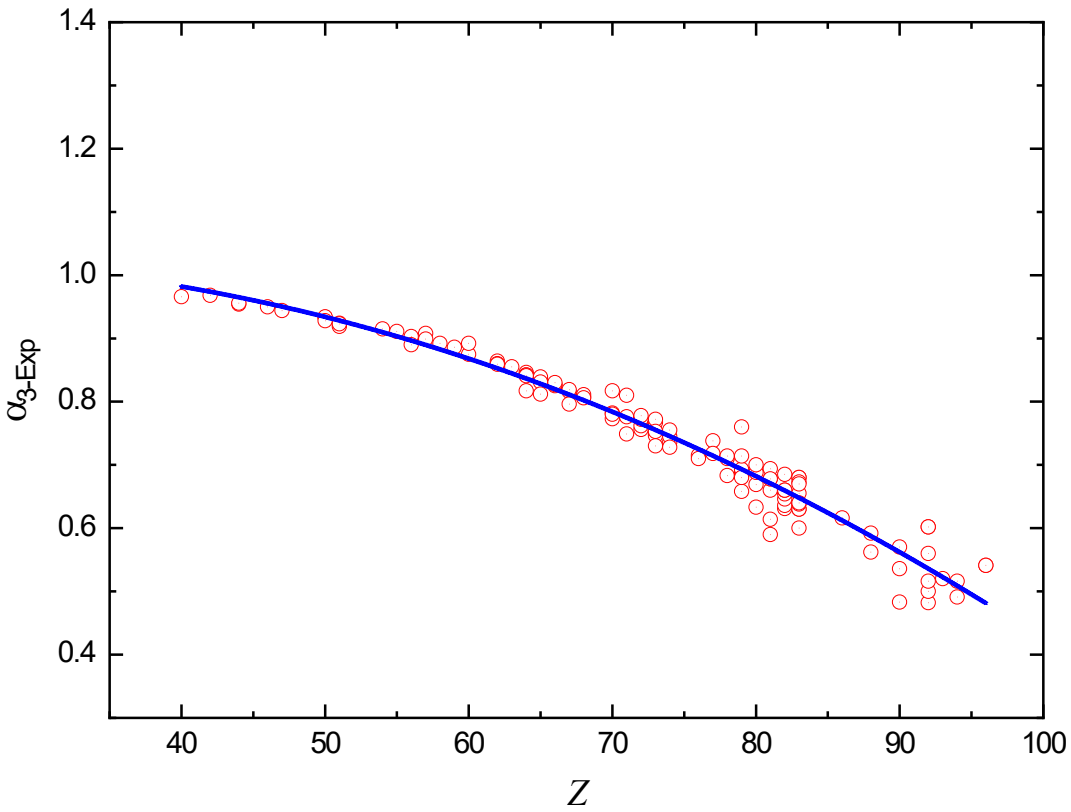

Figure 04:

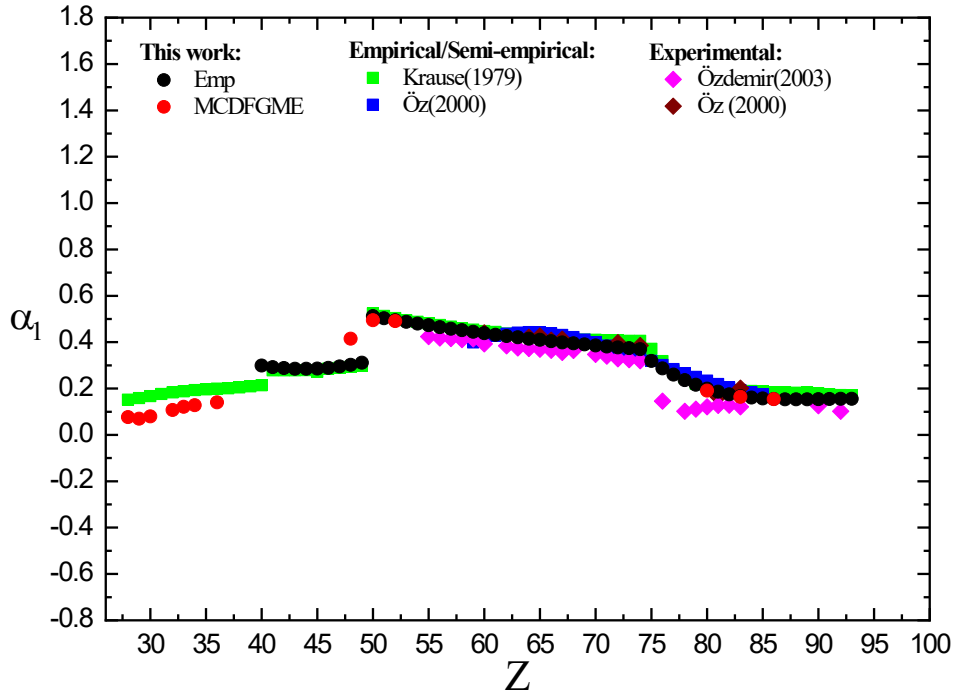
This work:
Emp
MCDFGME
Empirical/Semi-empirical:
Krause(1979)
Öz(2000)
Experimental:
Özdemir(2003)
Öz (2000)
α_1
Z
1.8
1.6
1.4
1.2
1.0
0.8
0.6
0.4
0.2
0.0
-0.2
-0.4
-0.6
-0.8
30
35
40
45
50
55
60
65
70
75
80
85
90
95
100

Figure 05:

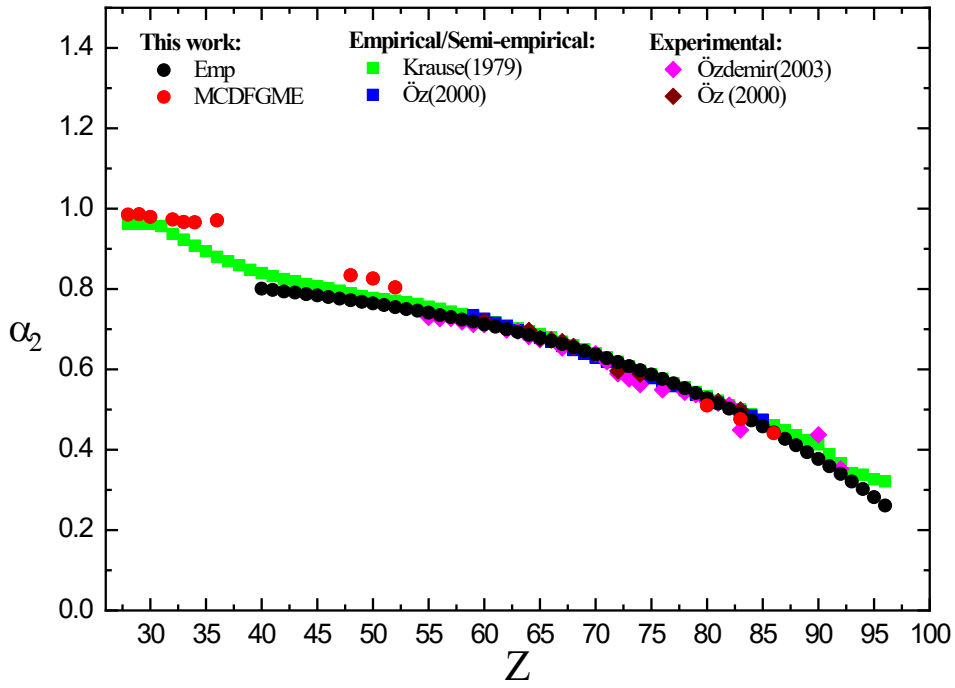
This work:
Emp
MCDFGME
Empirical/Semi-empirical:
Krause(1979)
Öz(2000)
Experimental:
Özdemir(2003)
Öz (2000)
α_2
Z
1.4
1.2
1.0
0.8
0.6
0.4
0.2
0.0
30
35
40
45
50
55
60
65
70
75
80
85
90
95
100

Figure 06:

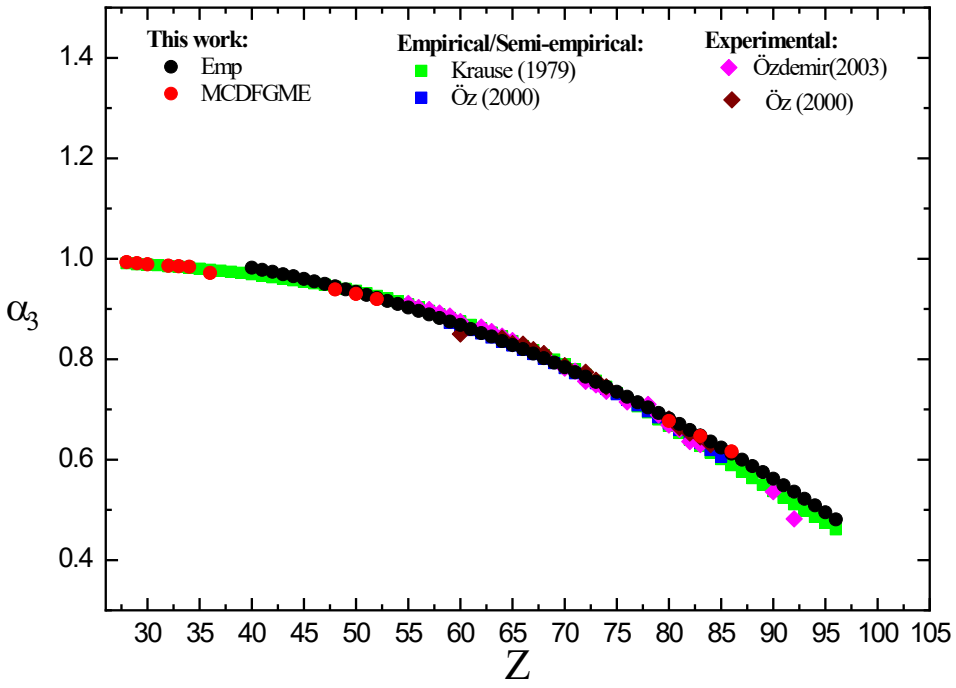
This work:
Emp
MCDFGME
Empirical/Semi-empirical:
Krause (1979)
Öz (2000)
Experimental:
Özdemir(2003)
Öz (2000)
α_3
Z
1.4
1.2
1.0
0.8
0.6
0.4
30 35 40 45 50 55 60 65 70 75 80 85 90 95 100 105

Table 1: Summary of fitting coefficients according to Eq. (1).

Auger decay parameter	**Z-group**	**Fit Parameters**	**Values**
a_1	$40 \leq Z \leq 49$	b_0	2.14952
		b_1	-0.08515
		b_2	9.71947×10^{-4}
		$\varepsilon_{RMS}(\%)$	=9.64
	$50 \leq Z \leq 74$	b_0	1.23473
		b_1	-0.0214
		b_2	1.3573×10^{-4}
		$\varepsilon_{RMS}(\%)$	=15.21
	$75 \leq Z \leq 92$	b_0	4.86193
		b_1	0.10141
		b_2	5.36508×10^{-4}
		$\varepsilon_{RMS}(\%)$	=25.46
a_2	$40 \leq Z \leq 96$	b_0	0.99695
		b_1	-0.00901
		b_2	1.6633×10^{-4}
		b_3	-1.58659×10^{-6}
		$\varepsilon_{RMS}(\%)$	=2.87
a_3	$40 \leq Z \leq 96$	b_0	0.9937
		b_1	0.0033
		b_2	-8.99703×10^{-5}
		$\varepsilon_{RMS}(\%)$	=0.60

Table 2: Empirical (this work), theoretical calculations, using the multiconfiguration Dirac-Fock method (MCDFGME), empirical, semi-empirical, and experimental (other works) of transition Auger a_1 from $_{28}$Ni to $_{93}$Np.

Z. element	This work		Other works		
			Empirical/semi-empirical		
	Emp	MCDFGME	Krause (1979)	Öz (2000)	Exp [a](Öz *et al*., 2000) [b](Özdemir, 2003)
$_{28}$Ni	-	0.0764	0.152	-	-
$_{29}$Cu	-	0.0698	0.159	-	-
$_{30}$Zn	-	0.0800	0.167	-	-
$_{31}$Ga	-	-	0.176	-	-
$_{32}$Ge	-	0.107	0.183	-	-
$_{33}$As	-	0.121	0.188	-	-
$_{34}$Se	-	0.128	0.193	-	-
$_{35}$Br	-	-	0.196	-	-
$_{36}$Kr	-	0.140	0.199	-	-
$_{37}$Rb	-	-	0.201	-	-
$_{38}$Sr	-	-	0.205	-	-
$_{39}$Y	-	-	0.209	-	-
$_{40}$Zr	0.299	-	0.214	-	-
$_{41}$Nb	0.292	-	0.278	-	-
$_{42}$Mo	0.288	-	0.278	-	-
$_{43}$Tc	0.285	-	0.278	-	-
$_{44}$Ru	0.285	-	0.279	-	-
$_{45}$Rh	0.286	-	0.272	-	-
$_{46}$Pd	0.289	-	0.286	-	-
$_{47}$Ag	0.295	-	0.29	-	-
$_{48}$Cd	0.302	0.415	0.294	-	-
$_{49}$In	0.311	-	0.299	-	-
$_{50}$Sn	0.512	0.495	0.524	-	-
$_{51}$Sb	0.503	-	0.513	-	-
$_{52}$Te	0.495	0.491	0.504	-	-
$_{53}$I	0.488	-	0.495	-	-
$_{54}$Xe	0.480	-	0.488	-	-
$_{55}$Cs	0.473	-	0.481		0.424[a]
$_{56}$Ba	0.465	-	0.474		0.418 [a]
$_{57}$La	0.458	-	0.467		0.416 [a]
$_{58}$Ce	0.452	-	0.46		0.411[a]
$_{59}$Pr	0.445	-	0.454	0.399	0.414[a]
$_{60}$Nd	0.439	-	0.448	0.415	0.393 [a],0.440[b]
$_{61}$Pm	0.432	-	0.444	0.427	-
$_{62}$Sm	0.426	-	0.437	0.436	0.384 [a]
$_{63}$Eu	0.421	-	0.432	0.441	0.375 [a]

$_{64}$Gd	0.415	-	0.428	0.443	0.373 [a], 0.422 [b]
$_{65}$Tb	0.410	-	0.424	0.442	0.370 [a], 0.426 [b]
$_{66}$Dy	0.404	-	0.419	0.438	0.365 [a], 0.409 [b]
$_{67}$Ho	0.399	-	0.416	0.431	0.356 [a], 0.413 [b]
$_{68}$Er	0.395	-	0.413	0.422	0.364 [a], 0.387 [b]
$_{69}$Tm	0.390	-	0.411	0.411	-
$_{70}$Yb	0.386	-	0.41	0.399	0.347 [a]
$_{71}$Lu	0.381	-	0.408	0.385	0.340 [a]
$_{72}$Hf	0.377	-	0.407	0.37	0.328 [a], 0.398 [b]
$_{73}$Ta	0.374	-	0.406	0.353	0.324 [a]
$_{74}$W	0.370	-	0.406	0.336	0.320 [a], 0.386 [b]
$_{75}$Re	0.319	-	0.371	0.319	
$_{76}$Os	0.287	-	0.318	0.301	0.146 [a]
$_{77}$Ir	0.260	-	0.277	0.284	
$_{78}$Pt	0.236	-	0.246	0.266	0.102 [a]
$_{79}$Au	0.216	-	0.221	0.25	0.111 [a]
$_{80}$Hg	0.199	0.191	0.203	0.234	0.121 [a]
$_{81}$Tl	0.186	-	0.197	0.219	0.127 [a], 0.164 [b]
$_{82}$PB	0.175	-	0.192	0.205	0.128 [a]
$_{83}$Bi	0.167	0.164	0.189	0.193	0.121 [a], 0.202 [b]
$_{84}$Po	0.161	-	0.189	0.183	-
$_{85}$At	0.157	-	0.187	0.175	-
$_{86}$Rn	0.155	0.154	0.184	-	-
$_{87}$Fr	0.153	-	0.184	-	-
$_{88}$Ra	0.153	-	0.182	-	-
$_{89}$Ac	0.153	-	0.183	-	-
$_{90}$Th	0.154	-	0.179	-	0.126 [a]
$_{91}$Pa	0.155	-	0.174	-	-
$_{92}$U	0.156	-	0.172	-	0.102 [a]
$_{93}$Np	0.156	-	0.171	-	-

Table 3: Empirical (this work), theoretical calculations, using the multiconfiguration Dirac-Fock method (MCDFGME), empirical, semi-empirical, and experimental (other works) of transition Auger a_2 from $_{28}$N to $_{96}$Cm.

Z. element	This work		Other works		
			Empirical/semi-empirical		
	Emp	MCDFGME	Krause (1979)	Öz (2000)	Exp [a] (Özdemir, 2003) [b](Öz *et al*., 2000)
$_{28}$Ni	-	0.985	0.963	-	-
$_{29}$Cu	-	0.986	0.962	-	-
$_{30}$Zn	-	0.979	0.963	-	-
$_{31}$Ga	-	-	0.956	-	-
$_{32}$Ge	-	0.973	0.937	-	-
$_{33}$As	-	0.967	0.923	-	-
$_{34}$Se	-	0.966	0.908	-	-
$_{35}$Br	-	-	0.894	-	-
$_{36}$Kr	-	0.971	0.88	-	-
$_{37}$Rb	-	-	0.869	-	-
$_{38}$Sr	-	-	0.859	-	-
$_{39}$Y	-	-	0.848	-	-
$_{40}$Zr	0.801	-	0.84	-	-
$_{41}$Nb	0.798	-	0.832	-	-
$_{42}$Mo	0.794	-	0.825	-	-
$_{43}$Tc	0.791	-	0.819	-	-
$_{44}$Ru	0.787	-	0.812	-	-
$_{45}$Rh	0.784	-	0.807	-	-
$_{46}$Pd	0.710	-	0.802	-	-
$_{47}$Ag	0.776	-	0.796	-	-
$_{48}$Cd	0.722	0.834	0.789	-	-
$_{49}$In	0.768	-	0.782	-	-
$_{50}$Sn	0.764	0.826	0.778	-	-
$_{51}$Sb	0.760	-	0.775	-	-
$_{52}$Te	0.755	0.804	0.771	-	-
$_{53}$I	0.750	-	0.767	-	-
$_{54}$Xe	0.746	-	0.763	-	-
$_{55}$Cs	0.741	-	0.756	-	0.729 [a]
$_{56}$Ba	0.735	-	0.751	-	0.726 [a]
$_{57}$La	0.730	-	0.744	-	0.727 [a]
$_{58}$Ce	0.724	-	0.737	-	0.718 [a]
$_{59}$Pr	0.719	-	0.73	0.735	0.712 [a]
$_{60}$Nd	0.712	-	0.724	0.726	0.711[a],0.720 [b]
$_{61}$Pm	0.706	-	0.717	0.716	-
$_{62}$Sm	0.700	-	0.71	0.707	0.698 [a]

$_{63}$Eu	0.639	-	0.702	0.697	0.695 [a]
$_{64}$Gd	0.686	-	0.695	0.687	0.682 [a],0.697 [b]
$_{65}$Tb	0.678	-	0.688	0.678	0.674 [a],0.677 [b]
$_{66}$Dy	0.671	-	0.679	0.668	0.674 [a], 0.673 [b]
$_{67}$Ho	0.663	-	0.669	0.658	0.653 [a], 0.669 [b]
$_{68}$Er	0.655	-	0.66	0.648	0.656 [a]
$_{69}$Tm	0.646	-	0.65	0.639	-
$_{70}$Yb	0.637	-	0.64	0.629	0.639 [a]
$_{71}$Lu	0.628	-	0.63	0.619	0.619 [a]
$_{72}$Hf	0.618	-	0.619	0.609	0.589 [a],0.596 [b]
$_{73}$Ta	0.608	-	0.608	0.599	0.576 [a]
$_{74}$W	0.598	-	0.597	0.589	0.562 [a],0.588 [b]
$_{75}$Re	0.587	-	0.587	0.578	-
$_{76}$Os	0.576	-	0.577	0.568	0.549 [a]
$_{77}$Ir	0.565	-	0.566	0.558	-
$_{78}$Pt	0.553	-	0.555	0.548	0.543 [a]
$_{79}$Au	0.541	-	0.544	0.537	0.537 [a]
$_{80}$Hg	0.528	0.510	0.533	0.527	0.520 [a]
$_{81}$Tl	0.515	-	0.522	0.517	0.516 [a],0.520 [b]
$_{82}$PB	0.502	-	0.511	0.506	0.511 [a]
$_{83}$Bi	0.488	0.476	0.5	0.496	0.449 [a],0.499 [b]
$_{84}$Po	0.473	-	0.488	0.485	-
$_{85}$At	0.458	-	0.474	0.475	-
$_{86}$Rn	0.443	0.441	0.401	-	-
$_{87}$Fr	0.427	-	0.448	-	-
$_{88}$Ra	0.411	-	0.436	-	-
$_{89}$Ac	0.394	-	0.424	-	-
$_{90}$Th	0.377	-	0.413	-	0.437 [a]
$_{91}$Pa	0.359	-	0.389	-	-
$_{92}$U	0.340	-	0.366	-	0.352 [a]
$_{93}$Np	0.321	-	0.342	-	-
$_{94}$Pu	0.302	-	0.338	-	-
$_{95}$Am	0.282	-	0.326	-	-
$_{96}$Cm	0.261	-	0.321	-	-

Table 4: Empirical (this work), theoretical calculations, using the multiconfiguration Dirac-Fock method (MCDFGME), empirical, semi-empirical, and experimental (other works) of transition Auger a_3 from $_{28}$N to $_{96}$Cm.

Z. element	This work		Other works		
			Empirical/semi-empirical		
	Emp	MCDFGME	Krause (1979)	Öz (2000)	Exp [a](Öz *et al*., 2000) [b](Özdemir, 2003)
$_{28}$Ni	-	0.993	0.991	-	-
$_{29}$Cu	-	0.991	0.989	-	-
$_{30}$Zn	-	0.989	0.988	-	-
$_{31}$Ga	-	-	0.987	-	-
$_{32}$Ge	-	0.986	0.985	-	
$_{33}$As	-	0.985	0.984	-	-
$_{34}$Se	-	0.984	0.982	-	-
$_{35}$Br	-	-	0.98	-	-
$_{36}$Kr	-	0.972	0.978	-	-
$_{37}$Rb	-	-	0.976	-	-
$_{38}$Sr	-	-	0.974	-	-
$_{39}$Y	-	-	0.972	-	-
$_{40}$Zr	0.982	-	0.969	-	-
$_{41}$Nb	0.978	-	0.966	-	-
$_{42}$Mo	0.974	-	0.963	-	-
$_{43}$Tc	0.969	-	0.96	-	-
$_{44}$Ru	0.965	-	0.957	-	
$_{45}$Rh	0.960	-	0.954	-	-
$_{46}$Pd	0.955	-	0.951	-	-
$_{47}$Ag	0.950	-	0.948	-	-
$_{48}$Cd	0.945	0.939	0.944	-	-
$_{49}$In	0.939	-	0.94	-	-
$_{50}$Sn	0.934	0.930	0.936	-	-
$_{51}$Sb	0.928	-	0.931	-	-
$_{52}$Te	0.922	0.920	0.926	-	-
$_{53}$I	0.916	-	0.921	-	-
$_{54}$Xe	0.910	-	0.915	-	-
$_{55}$Cs	0.903	-	0.909	-	0.911[b]
$_{56}$Ba	0.896	-	0.903	-	0.903[b]
$_{57}$La	0.889	-	0.896	-	0.899[b]
$_{58}$Ce	0.882	-	0.889	-	0.892[b]
$_{59}$Pr	0.875	-	0.882	0.872	0.886[b]
$_{60}$Nd	0.868	-	0.875	0.865	0875[b],0.850 [a]
$_{61}$Pm	0.860	-	0.868	0.858	-
$_{62}$Sm	0.852	-	0.861	0.851	0.864 [b]
$_{63}$Eu	0.845	-	0.853	0.843	0.855 [b]

$_{64}$Gd	0.836	-	0.845	0.835	0.846 [b],0.842 [a]
$_{65}$Tb	0.828	-	0.836	0.827	0.837 [b],0.831 [a]
$_{66}$Dy	0.820	-	0.826	0.819	0.825 [b] ,0.830 [a]
$_{67}$Ho	0.811	-	0.818	0.810	0.816 [b],0.819 [a]
$_{68}$Er	0.802	-	0.808	0.801	0.807 [b],0.811 [a]
$_{69}$Tm	0.793	-	0.799	0.792	-
$_{70}$Yb	0.784	-	0.79	0.782	0.782 [b],0.787 [a]
$_{71}$Lu	0.774	-	0.78	0.772	0.776 [b]
$_{72}$Hf	0.765	-	0.769	0.762	0.756 [b],0.774 [a]
$_{73}$Ta	0.755	-	0.757	0.752	0.749 [b],0.758 [a]
$_{74}$W	0.745	-	0.745	0.741	0.736 [b],0.745 [a]
$_{75}$Re	0.735	-	0.732	0.730	-
$_{76}$Os	0.725	-	0.719	0.719	0.715 [b]
$_{77}$Ir	0.714	-	0.706	0.708	-
$_{78}$Pt	0.704	-	0.694	0.696	0.710[b]
$_{79}$Au	0.693	-	0.68	0.684	0.689[b],0.681 [a]
$_{80}$Hg	0.682	0.677	0.667	0.672	0.669[b],0.664 [a]
$_{81}$Tl	0.671	-	0.653	0.659	0.660[b],0.653 [a]
$_{82}$PB	0.659	-	0.64	0.646	0.636[b],0.645 [a]
$_{83}$Bi	0.648	0.647	0.627	0.633	0.630[b],0.630 [a]
$_{84}$Po	0.636	-	0.614	0.619	-
$_{85}$At	0.624	-	0.601	0.606	-
$_{86}$Rn	0.612	0.616	0.589	-	-
$_{87}$Fr	0.600	-	0.576	-	-
$_{88}$Ra	0.587	-	0.563	-	-
$_{89}$Ac	0.575	-	0.55	-	-
$_{90}$Th	0.562	-	0.537	-	0.536[b]
$_{91}$Pa	0.549	-	0.524	-	-
$_{92}$U	0.536	-	0.511	-	0.482[b]
$_{93}$Np	0.522	-	0.498	-	-
$_{94}$Pu	0.509	-	0.486	-	-
$_{95}$Am	0.495	-	0.474	-	-
$_{96}$Cm	0.481	-	0.461	-	-